Measurement of Branching Fractions and Resonance Contributions for $B^0 \to \bar{D}^0 K^+ \pi^-$ and Search for $B^0 \to D^0 K^+ \pi^-$ Decays

B. Aubert,[1] R. Barate,[1] D. Boutigny,[1] F. Couderc,[1] Y. Karyotakis,[1] J. P. Lees,[1] V. Poireau,[1] V. Tisserand,[1] A. Zghiche,[1] E. Grauges,[2] A. Palano,[3] M. Pappagallo,[3] A. Pompili,[3] J. C. Chen,[4] N. D. Qi,[4] G. Rong,[4] P. Wang,[4] Y. S. Zhu,[4] G. Eigen,[5] I. Ofte,[5] B. Stugu,[5] G. S. Abrams,[6] M. Battaglia,[6] D. Best,[6] A. B. Breon,[6] D. N. Brown,[6] J. Button-Shafer,[6] R. N. Cahn,[6] E. Charles,[6] C. T. Day,[6] M. S. Gill,[6] A. V. Gritsan,[6] Y. Groysman,[6] R. G. Jacobsen,[6] R. W. Kadel,[6] J. Kadyk,[6] L. T. Kerth,[6] Yu. G. Kolomensky,[6] G. Kukartsev,[6] G. Lynch,[6] L. M. Mir,[6] P. J. Oddone,[6] T. J. Orimoto,[6] M. Pripstein,[6] N. A. Roe,[6] M. T. Ronan,[6] W. A. Wenzel,[6] M. Barrett,[7] K. E. Ford,[7] T. J. Harrison,[7] A. J. Hart,[7] C. M. Hawkes,[7] S. E. Morgan,[7] A. T. Watson,[7] M. Fritsch,[8] K. Goetzen,[8] T. Held,[8] H. Koch,[8] B. Lewandowski,[8] M. Pelizaeus,[8] K. Peters,[8] T. Schroeder,[8] M. Steinke,[8] J. T. Boyd,[9] J. P. Burke,[9] N. Chevalier,[9] W. N. Cottingham,[9] T. Cuhadar-Donszelmann,[10] B. G. Fulsom,[10] C. Hearty,[10] N. S. Knecht,[10] T. S. Mattison,[10] J. A. McKenna,[10] A. Khan,[11] P. Kyberd,[11] M. Saleem,[11] L. Teodorescu,[11] A. E. Blinov,[12] V. E. Blinov,[12] A. D. Bukin,[12] V. P. Druzhinin,[12] V. B. Golubev,[12] E. A. Kravchenko,[12] A. P. Onuchin,[12] S. I. Serednyakov,[12] Yu. I. Skovpen,[12] E. P. Solodov,[12] A. N. Yushkov,[12] M. Bondioli,[13] M. Bruinsma,[13] M. Chao,[13] S. Curry,[13] I. Eschrich,[13] D. Kirkby,[13] A. J. Lankford,[13] P. Lund,[13] M. Mandelkern,[13] R. K. Mommsen,[13] W. Roethel,[13] D. P. Stoker,[13] C. Buchanan,[14] B. L. Hartfiel,[14] S. D. Foulkes,[15] J. W. Gary,[15] O. Long,[15] B. C. Shen,[15] K. Wang,[15] L. Zhang,[15] D. del Re,[16] H. K. Hadavand,[16] E. J. Hill,[16] D. B. MacFarlane,[16] H. P. Paar,[16] S. Rahatlou,[16] V. Sharma,[16] J. W. Berryhill,[17] C. Campagnari,[17] A. Cunha,[17] B. Dahmes,[17] T. M. Hong,[17] M. A. Mazur,[17] J. D. Richman,[17] W. Verkerke,[17] T. W. Beck,[18] A. M. Eisner,[18] C. J. Flacco,[18] C. A. Heusch,[18] J. Kroseberg,[18] W. S. Lockman,[18] G. Nesom,[18] T. Schalk,[18] B. A. Schumm,[18] A. Seiden,[18] P. Spradlin,[18] D. C. Williams,[18] M. G. Wilson,[18] J. Albert,[19] E. Chen,[19] G. P. Dubois-Felsmann,[19] A. Dvoretskii,[19] D. G. Hitlin,[19] J. S. Minamora,[19] I. Narsky,[19] T. Piatenko,[19] F. C. Porter,[19] A. Ryd,[19] A. Samuel,[19] R. Andreassen,[20] G. Mancinelli,[20] B. T. Meadows,[20] M. D. Sokoloff,[20] F. Blanc,[21] P. C. Bloom,[21] S. Chen,[21] W. T. Ford,[21] J. F. Hirschauer,[21] A. Kreisel,[21] U. Nauenberg,[21] A. Olivas,[21] W. O. Ruddick,[21] J. G. Smith,[21] K. A. Ulmer,[21] S. R. Wagner,[21] J. Zhang,[21] A. Chen,[22] E. A. Eckhart,[22] A. Soffer,[22] W. H. Toki,[22] R. J. Wilson,[22] Q. Zeng,[22] D. Altenburg,[23] E. Feltresi,[23] A. Hauke,[23] B. Spaan,[23] T. Brandt,[24] J. Brose,[24] M. Dickopp,[24] V. Klose,[24] H. M. Lacker,[24] R. Nogowski,[24] S. Otto,[24] A. Petzold,[24] J. Schubert,[24] K. R. Schubert,[24] R. Schwierz,[24] J. E. Sundermann,[24] D. Bernard,[25] G. R. Bonneaud,[25] P. Grenier,[25] S. Schrenk,[25] Ch. Thiebaux,[25] G. Vasileiadis,[25] M. Verderi,[25] D. J. Bard,[26] P. J. Clark,[26] W. Gradl,[26] F. Muheim,[26] S. Playfer,[26] Y. Xie,[26] M. Andreotti,[27] D. Bettoni,[27] C. Bozzi,[27] R. Calabrese,[27] G. Cibinetto,[27] E. Luppi,[27] M. Negrini,[27] L. Piemontese,[27] F. Anulli,[28] R. Baldini-Ferroli,[28] A. Calcaterra,[28] R. de Sangro,[28] G. Finocchiaro,[28] P. Patteri,[28] I. M. Peruzzi,[28,*] M. Piccolo,[28] A. Zallo,[28] A. Buzzo,[29] R. Capra,[29] R. Contri,[29] M. Lo Vetere,[29] M. M. Macri,[29] M. R. Monge,[29] S. Passaggio,[29] C. Patrignani,[29] E. Robutti,[29] A. Santroni,[29] S. Tosi,[29] G. Brandenburg,[30] K. S. Chaisanguanthum,[30] M. Morii,[30] E. Won,[30] J. Wu,[30] R. S. Dubitzky,[31] U. Langenegger,[31] J. Marks,[31] S. Schenk,[31] U. Uwer,[31] W. Bhimji,[32] D. A. Bowerman,[32] P. D. Dauncey,[32] U. Egede,[32] R. L. Flack,[32] J. R. Gaillard,[32] J . A. Nash,[32] M. B. Nikolich,[32] W. Panduro Vazquez,[32] X. Chai,[33] M. J. Charles,[33] W. F. Mader,[33] U. Mallik,[33] V. Ziegler,[33] J. Cochran,[34] H. B. Crawley,[34] V. Eyges,[34] W. T. Meyer,[34] S. Prell,[34] E. I. Rosenberg,[34] A. E. Rubin,[34] J. I. Yi,[34] G. Schott,[35] N. Arnaud,[36] M. Davier,[36] X. Giroux,[36] G. Grosdidier,[36] A. Höcker,[36] F. Le Diberder,[36] V. Lepeltier,[36] A. M. Lutz,[36] A. Oyanguren,[36] T. C. Petersen,[36] S. Plaszczynski,[36] S. Rodier,[36] P. Roudeau,[36] M. H. Schune,[36] A. Stocchi,[36] G. Wormser,[36] C. H. Cheng,[37] D. J. Lange,[37] M. C. Simani,[37] D. M. Wright,[37] A. J. Bevan,[38] C. A. Chavez,[38] I. J. Forster,[38] J. R. Fry,[38] E. Gabathuler,[38] R. Gamet,[38] K. A. George,[38] D. E. Hutchcroft,[38] R. J. Parry,[38] D. J. Payne,[38] K. C. Schofield,[38] C. Touramanis,[38] C. M. Cormack,[39] F. Di Lodovico,[39] W. Menges,[39] R. Sacco,[39] C. L. Brown,[40] G. Cowan,[40] H. U. Flaecher,[40] M. G. Green,[40] D. A. Hopkins,[40] P. S. Jackson,[40] T. R. McMahon,[40] S. Ricciardi,[40] F. Salvatore,[40] D. N. Brown,[41] C. L. Davis,[41] J. Allison,[42] N. R. Barlow,[42] R. J. Barlow,[42] C. L. Edgar,[42] M. C. Hodgkinson,[42] M. P. Kelly,[42] G. D. Lafferty,[42] M. T. Naisbit,[42] J. C. Williams,[42] C. Chen,[43] W. D. Hulsbergen,[43] A. Jawahery,[43] D. Kovalskyi,[43] C. K. Lae,[43] D. A. Roberts,[43] G. Simi,[43] G. Blaylock,[44] C. Dallapiccola,[44] S. S. Hertzbach,[44] R. Kofler,[44] X. Li,[44] T. B. Moore,[44] S. Saremi,[44] H. Staengle,[44] S. Y. Willocq,[44] R. Cowan,[45] K. Koeneke,[45] G. Sciolla,[45] S. J. Sekula,[45] M. Spitznagel,[45] F. Taylor,[45] R. K. Yamamoto,[45] H. Kim,[46] P. M. Patel,[46] S. H. Robertson,[46] A. Lazzaro,[47] V. Lombardo,[47] F. Palombo,[47] J. M. Bauer,[48] L. Cremaldi,[48] V. Eschenburg,[48] R. Godang,[48] R. Kroeger,[48] J. Reidy,[48] D. A. Sanders,[48] D. J. Summers,[48] H. W. Zhao,[48] S. Brunet,[49] D. Côté,[49] P. Taras,[49] F. B. Viaud,[49] H. Nicholson,[50] N. Cavallo,[51] G. De Nardo,[51] F. Fabozzi,[51,†] C. Gatto,[51] L. Lista,[51] D. Monorchio,[51] P. Paolucci,[51] D. Piccolo,[51] C. Sciacca,[51] M. Baak,[52] H. Bulten,[52] G. Raven,[52] H. L. Snoek,[52] L. Wilden,[52]

C. P. Jessop,[53] J. M. LoSecco,[53] T. Allmendinger,[54] G. Benelli,[54] K. K. Gan,[54] K. Honscheid,[54] D. Hufnagel,[54] P. D. Jackson,[54] H. Kagan,[54] R. Kass,[54] T. Pulliam,[54] A. M. Rahimi,[54] R. Ter-Antonyan,[54] Q. K. Wong,[54] N. L. Blount,[55] J. Brau,[55] R. Frey,[55] O. Igonkina,[55] M. Lu,[55] C. T. Potter,[55] R. Rahmat,[55] N. B. Sinev,[55] D. Strom,[55] J. Strube,[55] E. Torrence,[55] F. Galeazzi,[56] M. Margoni,[56] M. Morandin,[56] M. Posocco,[56] M. Rotondo,[56] F. Simonetto,[56] R. Stroili,[56] C. Voci,[56] M. Benayoun,[57] H. Briand,[57] J. Chauveau,[57] P. David,[57] L. Del Buono,[57] Ch. de la Vaissière,[57] O. Hamon,[57] M. J. J. John,[57] Ph. Leruste,[57] J. Malclès,[57] J. Ocariz,[57] L. Roos,[57] G. Therin,[57] P. K. Behera,[58] L. Gladney,[58] Q. H. Guo,[58] J. Panetta,[58] M. Biasini,[59] R. Covarelli,[59] S. Pacetti,[59] M. Pioppi,[59] C. Angelini,[60] G. Batignani,[60] S. Bettarini,[60] F. Bucci,[60] G. Calderini,[60] M. Carpinelli,[60] R. Cenci,[60] F. Forti,[60] M. A. Giorgi,[60] A. Lusiani,[60] G. Marchiori,[60] M. Morganti,[60] N. Neri,[60] E. Paoloni,[60] M. Rama,[60] G. Rizzo,[60] J. Walsh,[60] M. Haire,[61] D. Judd,[61] D. E. Wagoner,[61] J. Biesiada,[62] N. Danielson,[62] P. Elmer,[62] Y. P. Lau,[62] C. Lu,[62] J. Olsen,[62] A. J. S. Smith,[62] A. V. Telnov,[62] F. Bellini,[63] G. Cavoto,[63] A. D'Orazio,[63] E. Di Marco,[63] R. Faccini,[63] F. Ferrarotto,[63] F. Ferroni,[63] M. Gaspero,[63] L. Li Gioi,[63] M. A. Mazzoni,[63] S. Morganti,[63] G. Piredda,[63] F. Polci,[63] F. Safai Tehrani,[63] C. Voena,[63] H. Schröder,[64] R. Waldi,[64] T. Adye,[65] N. De Groot,[65] B. Franek,[65] G. P. Gopal,[65] E. O. Olaiya,[65] F. F. Wilson,[65] R. Aleksan,[66] S. Emery,[66] A. Gaidot,[66] S. F. Ganzhur,[66] G. Graziani,[66] G. Hamel de Monchenault,[66] W. Kozanecki,[66] M. Legendre,[66] G. W. London,[66] B. Mayer,[66] G. Vasseur,[66] Ch. Yèche,[66] M. Zito,[66] M. V. Purohit,[67] A. W. Weidemann,[67] J. R. Wilson,[67] F. X. Yumiceva,[67] T. Abe,[68] M. T. Allen,[68] D. Aston,[68] R. Bartoldus,[68] N. Berger,[68] A. M. Boyarski,[68] O. L. Buchmueller,[68] R. Claus,[68] J. P. Coleman,[68] M. R. Convery,[68] M. Cristinziani,[68] J. C. Dingfelder,[68] D. Dong,[68] J. Dorfan,[68] D. Dujmic,[68] W. Dunwoodie,[68] S. Fan,[68] R. C. Field,[68] T. Glanzman,[68] S. J. Gowdy,[68] T. Hadig,[68] V. Halyo,[68] C. Hast,[68] T. Hryn'ova,[68] W. R. Innes,[68] M. H. Kelsey,[68] P. Kim,[68] M. L. Kocian,[68] D. W. G. S. Leith,[68] J. Libby,[68] S. Luitz,[68] V. Luth,[68] H. L. Lynch,[68] H. Marsiske,[68] R. Messner,[68] D. R. Muller,[68] C. P. O'Grady,[68] V. E. Ozcan,[68] A. Perazzo,[68] M. Perl,[68] B. N. Ratcliff,[68] A. Roodman,[68] A. A. Salnikov,[68] R. H. Schindler,[68] J. Schwiening,[68] A. Snyder,[68] J. Stelzer,[68] D. Su,[68] M. K. Sullivan,[68] K. Suzuki,[68] S. K. Swain,[68] J. M. Thompson,[68] J. Va'vra,[68] N. van Bakel,[68] M. Weaver,[68] A. J. R. Weinstein,[68] W. J. Wisniewski,[68] M. Wittgen,[68] D. H. Wright,[68] A. K. Yarritu,[68] K. Yi,[68] C. C. Young,[68] P. R. Burchat,[69] A. J. Edwards,[69] S. A. Majewski,[69] B. A. Petersen,[69] C. Roat,[69] M. Ahmed,[70] S. Ahmed,[70] M. S. Alam,[70] R. Bula,[70] J. A. Ernst,[70] M. A. Saeed,[70] F. R. Wappler,[70] S. B. Zain,[70] W. Bugg,[71] M. Krishnamurthy,[71] S. M. Spanier,[71] R. Eckmann,[72] J. L. Ritchie,[72] A. Satpathy,[72] R. F. Schwitters,[72] J. M. Izen,[73] I. Kitayama,[73] X. C. Lou,[73] S. Ye,[73] F. Bianchi,[74] M. Bona,[74] F. Gallo,[74] D. Gamba,[74] M. Bomben,[75] L. Bosisio,[75] C. Cartaro,[75] F. Cossutti,[75] G. Della Ricca,[75] S. Dittongo,[75] S. Grancagnolo,[75] L. Lanceri,[75] L. Vitale,[75] V. Azzolini,[76] F. Martinez-Vidal,[76] R. S. Panvini,[77,‡] Sw. Banerjee,[78] B. Bhuyan,[78] C. M. Brown,[78] D. Fortin,[78] K. Hamano,[78] R. Kowalewski,[78] J. M. Roney,[78] R. J. Sobie,[78] J. J. Back,[79] P. F. Harrison,[79] T. E. Latham,[79] G. B. Mohanty,[79] H. R. Band,[80] X. Chen,[80] B. Cheng,[80] S. Dasu,[80] M. Datta,[80] A. M. Eichenbaum,[80] K. T. Flood,[80] M. T. Graham,[80] J. J. Hollar,[80] J. R. Johnson,[80] P. E. Kutter,[80] H. Li,[80] R. Liu,[80] B. Mellado,[80] A. Mihalyi,[80] A. K. Mohapatra,[80] Y. Pan,[80] M. Pierini,[80] R. Prepost,[80] P. Tan,[80] S. L. Wu,[80] Z. Yu,[80] and H. Neal[81]

(The *BABAR* Collaboration)

[1]*Laboratoire de Physique des Particules, F-74941 Annecy-le-Vieux, France*
[2]*IFAE, Universitat Autonoma de Barcelona, E-08193 Bellaterra, Barcelona, Spain*
[3]*Università di Bari, Dipartimento di Fisica and INFN, I-70126 Bari, Italy*
[4]*Institute of High Energy Physics, Beijing 100039, China*
[5]*University of Bergen, Institute of Physics, N-5007 Bergen, Norway*
[6]*Lawrence Berkeley National Laboratory and University of California, Berkeley, California 94720, USA*
[7]*University of Birmingham, Birmingham, B15 2TT, United Kingdom*
[8]*Ruhr Universität Bochum, Institut für Experimentalphysik 1, D-44780 Bochum, Germany*
[9]*University of Bristol, Bristol BS8 1TL, United Kingdom*
[10]*University of British Columbia, Vancouver, British Columbia, Canada V6T 1Z1*
[11]*Brunel University, Uxbridge, Middlesex UB8 3PH, United Kingdom*
[12]*Budker Institute of Nuclear Physics, Novosibirsk 630090, Russia*
[13]*University of California at Irvine, Irvine, California 92697, USA*
[14]*University of California at Los Angeles, Los Angeles, California 90024, USA*
[15]*University of California at Riverside, Riverside, California 92521, USA*
[16]*University of California at San Diego, La Jolla, California 92093, USA*
[17]*University of California at Santa Barbara, Santa Barbara, California 93106, USA*
[18]*Institute for Particle Physics, University of California at Santa Cruz, Santa Cruz, California 95064, USA*

[19]California Institute of Technology, Pasadena, California 91125, USA
[20]University of Cincinnati, Cincinnati, Ohio 45221, USA
[21]University of Colorado, Boulder, Colorado 80309, USA
[22]Colorado State University, Fort Collins, Colorado 80523, USA
[23]Universität Dortmund, Institut für Physik, D-44221 Dortmund, Germany
[24]Technische Universität Dresden, Institut für Kern- und Teilchenphysik, D-01062 Dresden, Germany
[25]Ecole Polytechnique, LLR, F-91128 Palaiseau, France
[26]University of Edinburgh, Edinburgh EH9 3JZ, United Kingdom
[27]Università di Ferrara, Dipartimento di Fisica and INFN, I-44100 Ferrara, Italy
[28]Laboratori Nazionali di Frascati dell'INFN, I-00044 Frascati, Italy
[29]Università di Genova, Dipartimento di Fisica and INFN, I-16146 Genova, Italy
[30]Harvard University, Cambridge, Massachusetts 02138, USA
[31]Universität Heidelberg, Physikalisches Institut, Philosophenweg 12, D-69120 Heidelberg, Germany
[32]Imperial College London, London, SW7 2AZ, United Kingdom
[33]University of Iowa, Iowa City, Iowa 52242, USA
[34]Iowa State University, Ames, Iowa 50011-3160, USA
[35]Universität Karlsruhe, Institut für Experimentelle Kernphysik, D-76021 Karlsruhe, Germany
[36]Laboratoire de l'Accélérateur Linéaire, F-91898 Orsay, France
[37]Lawrence Livermore National Laboratory, Livermore, California 94550, USA
[38]University of Liverpool, Liverpool L69 72E, United Kingdom
[39]Queen Mary, University of London, E1 4NS, United Kingdom
[40]University of London, Royal Holloway and Bedford New College, Egham, Surrey TW20 0EX, United Kingdom
[41]University of Louisville, Louisville, Kentucky 40292, USA
[42]University of Manchester, Manchester M13 9PL, United Kingdom
[43]University of Maryland, College Park, Maryland 20742, USA
[44]University of Massachusetts, Amherst, Massachusetts 01003, USA
[45]Laboratory for Nuclear Science, Massachusetts Institute of Technology, Cambridge, Massachusetts 02139, USA
[46]McGill University, Montréal, Québec, Canada H3A 2T8
[47]Università di Milano, Dipartimento di Fisica and INFN, I-20133 Milano, Italy
[48]University of Mississippi, University, Mississippi 38677, USA
[49]Université de Montréal, Physique des Particules, Montréal, Québec, Canada H3C 3J7
[50]Mount Holyoke College, South Hadley, Massachusetts 01075, USA
[51]Università di Napoli Federico II, Dipartimento di Scienze Fisiche and INFN, I-80126, Napoli, Italy
[52]NIKHEF, National Institute for Nuclear Physics and High Energy Physics, NL-1009 DB Amsterdam, The Netherlands
[53]University of Notre Dame, Notre Dame, Indiana 46556, USA
[54]Ohio State University, Columbus, Ohio 43210, USA
[55]University of Oregon, Eugene, Oregon 97403, USA
[56]Università di Padova, Dipartimento di Fisica and INFN, I-35131 Padova, Italy
[57]Universités Paris VI et VII, Laboratoire de Physique Nucléaire et de Hautes Energies, F-75252 Paris, France
[58]University of Pennsylvania, Philadelphia, Pennsylvania 19104, USA
[59]Università di Perugia, Dipartimento di Fisica and INFN, I-06100 Perugia, Italy
[60]Dipartimento di Fisica, Scuola Normale Superiore, Università di Pisa and INFN, I-56127 Pisa, Italy
[61]Prairie View A&M University, Prairie View, Texas 77446, USA
[62]Princeton University, Princeton, New Jersey 08544, USA
[63]Università di Roma La Sapienza, Dipartimento di Fisica and INFN, I-00185 Roma, Italy
[64]Universität Rostock, D-18051 Rostock, Germany
[65]Rutherford Appleton Laboratory, Chilton, Didcot, Oxon, OX11 0QX, United Kingdom
[66]DSM/Dapnia, CEA/Saclay, F-91191 Gif-sur-Yvette, France
[67]University of South Carolina, Columbia, South Carolina 29208, USA
[68]Stanford Linear Accelerator Center, Stanford, California 94309, USA
[69]Stanford University, Stanford, California 94305-4060, USA
[70]State University of New York, Albany, New York 12222, USA
[71]University of Tennessee, Knoxville, Tennessee 37996, USA
[72]University of Texas at Austin, Austin, Texas 78712, USA
[73]University of Texas at Dallas, Richardson, Texas 75083, USA
[74]Dipartimento di Fisica Sperimentale, Università di Torino and INFN, I-10125 Torino, Italy
[75]Dipartimento di Fisica, Università di Trieste and INFN, I-34127 Trieste, Italy
[76]IFIC, Universitat de Valencia-CSIC, E-46071 Valencia, Spain
[77]Vanderbilt University, Nashville, Tennessee 37235, USA
[78]University of Victoria, Victoria, British Columbia, Canada V8W 3P6
[79]Department of Physics, University of Warwick, Coventry CV4 7AL, United Kingdom

[80]University of Wisconsin, Madison, Wisconsin 53706, USA
[81]Yale University, New Haven, Connecticut 06511, USA
(Received 23 September 2005; published 11 January 2006)

Using 226×10^6 $\Upsilon(4S) \to B\bar{B}$ events collected with the *BABAR* detector at the PEP-II e^+e^- storage ring at the Stanford Linear Accelerator Center, we measure the branching fraction for $B^0 \to \bar{D}^0 K^+ \pi^-$, excluding $B^0 \to D^{*-} K^+$, to be $\mathcal{B}(B^0 \to \bar{D}^0 K^+ \pi^-) = (88 \pm 15 \pm 9) \times 10^{-6}$. We observe $B^0 \to \bar{D}^0 K^*(892)^0$ and $B^0 \to D_2^*(2460)^- K^+$ contributions. The ratio of branching fractions $\mathcal{B}(B^0 \to D^{*-} K^+)/\mathcal{B}(B^0 \to D^{*-} \pi^+) = (7.76 \pm 0.34 \pm 0.29)\%$ is measured separately. The branching fraction for the suppressed mode $B^0 \to D^0 K^+ \pi^-$ is $\mathcal{B}(B^0 \to D^0 K^+ \pi^-) < 19 \times 10^{-6}$ at the 90% confidence level.

DOI: 10.1103/PhysRevLett.96.011803 PACS numbers: 13.25.Hw

A theoretically clean method for measuring the angle $\gamma = \arg(-V_{ud}V_{ub}^*/V_{cd}V_{cb}^*)$ in the unitarity triangle of the Cabibbo-Kobayashi-Maskawa (CKM) quark-mixing matrix [1] in the standard model of particle physics utilizes decay modes of the type $B \to DK$. Several methods have been proposed [2–4] to extract γ from these decays using interference effects between $b \to u\bar{c}s$ and $b \to c\bar{u}s$ processes. However, the $b \to u\bar{c}s$ amplitude is suppressed by a color factor in addition to the CKM factor $|V_{ub}V_{cs}^*/V_{cb}V_{us}^*| \simeq 0.4$, and the extraction of γ with previous methods in Refs. [2,3] is subject to an eightfold ambiguity due to unknown strong phases.

Three-body $B \to DK\pi$ decays have been proposed [5,6] as an alternative method for measuring γ. In these modes, the CKM-suppressed $b \to u\bar{c}s$ processes include color-allowed diagrams; thus larger decay rates and more significant *CP* violation effects are possible. In addition, a $DK\pi$ Dalitz plot analysis can resolve the strong phase and reduce the ambiguity to twofold, similar to Ref. [4]. The sensitivity to γ in these decays is determined by the size of the overlapping $b \to c\bar{u}s$ and $b \to u\bar{c}s$ amplitudes in the Dalitz plot.

In this Letter, we report the measurements of the branching fraction for the CKM-favored $B^0 \to \bar{D}^0 K^+ \pi^-$ [7] decay and dominant resonance contributions, and the search for the CKM-suppressed $B^0 \to D^0 K^+ \pi^-$ decays. The flavor of the B meson is tagged by the charge of the prompt kaon. The favored mode has been previously observed through its dominant resonances $D^{*-}K^+$ [8] and $\bar{D}^0 K^*(892)^0$ [9]. Since $D^{*-}K^+$ occupies only a very small region of the allowed phase space, we treat it separately and measure the ratio $r = \mathcal{B}(B^0 \to D^{*-} K^+)/\mathcal{B}(B^0 \to D^{*-}\pi^+)$, which can be used to test factorization and flavor-SU(3) symmetry.

Signal events are selected from 226×10^6 $B\bar{B}$pairs collected with the *BABAR* detector [10] at the PEP-II asymmetric-energy storage ring. Charged tracks are detected by a five-layer silicon vertex tracker and a 40-layer drift chamber. Hadrons are identified based on the ionization energy loss in the tracking system and the opening angle of the Cherenkov radiation in a ring-image detector [11]. Photons are measured by an electromagnetic calorimeter. These systems are mounted inside a 1.5 T solenoidal superconducting magnet.

The D^0 candidate is reconstructed through $K^-\pi^+$, $K^-\pi^+\pi^0$, and $K^-\pi^+\pi^-\pi^+$ channels, where the measured invariant mass is required to be within 20, 35, and 20 MeV/c^2, respectively, of the nominal D^0 mass [12], corresponding to 3.0, 2.5, and 3.0 σ. A vertex fit is performed with the mass constrained to the nominal value. The π^0 candidate is formed from two photon candidates with invariant mass between 115 and 150 MeV/c^2.

For the measurement of the ratio r, the D^0 is combined with a low momentum π to form a D^* candidate, with its vertex constrained to the interaction point (beam spot). Candidates with mass difference $m_{D^0\pi} - m_{D^0}$ between 144 and 147 MeV/c^2 are retained. A charged track, assumed to have the pion mass, is combined with the D^* to form a B^0 candidate. The χ^2 probabilities for both the D^* and B^0 vertex fits are required to be greater than 0.1%. To reject jetlike continuum background, the normalized Fox-Wolfram second moment R_2 [13], computed with charged tracks and neutral clusters, is required to be less than 0.5, and $|\cos\theta_T|$ less than 0.85, where θ_T is the thrust angle between the B^0 candidate and the rest of the event in the e^+e^- center-of-mass (c.m.) frame.

For $B^0 \to \bar{D}^0 K^+ \pi^-$ and $D^0 K^+ \pi^-$ measurements, the B^0 candidate is formed by combining a D^0 candidate with oppositely charged pion and kaon candidates. We select candidates outside the $D^{*-}K^+$ region ($142.5 < m_{D^0\pi} - m_{D^0} < 148.5$ MeV/c^2, a 6σ window). The measured D^0 invariant mass must be within 12, 28, and 8.5 MeV/c^2 of the nominal D^0 mass for $K\pi$, $K\pi\pi^0$, and $K\pi\pi\pi$ modes, respectively. Candidates are rejected if the $D^0 \to K\pi\pi^0$ decay probability, computed with the Dalitz parameters measured in Ref. [14], is less than 6% of the maximum value. The χ^2 probability of the D^0 (B^0) vertex fit is required to be greater than 0.5% (2%). All charged tracks are required to have at least 12 hits in the drift chamber and transverse momentum greater than 100 MeV/c. Both kaon candidates are required to be consistent with the kaon hypothesis. Prompt pion candidates consistent with the kaon hypothesis are rejected.

To further reduce the continuum background, $|\cos\theta_B^*|$ must be less than 0.9, where θ_B^* is the polar angle of the B^0 candidate in the c.m. frame. A Fisher discriminant $\mathcal{F}$ is formed based on R_2, $\cos\theta_T$, θ_B^*, and two moments L_0 and L_2, where $L_i = \sum_j p_j^* |\cos\theta_j^*|^i$, summed over the remaining

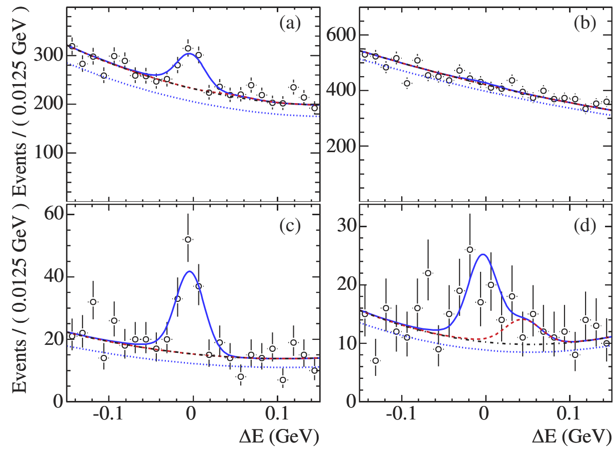

FIG. 1 (color online). ΔE distributions and PDF projections with $m_{\rm ES} > 5.27\ {\rm GeV}/c^2$ for (a) $B^0 \to \bar{D}^0 K^+ \pi^-$ excluding $D^{*-}K^+$ candidates, (b) $B^0 \to D^0 K^+ \pi^-$, (c) $B^0 \to \bar{D}^0 K^*(892)^0$, and (d) $B^0 \to D_2^*(2460)^- K^+$, for the three D^0 modes combined. Circles with error bars are data points. Four curves from top to bottom represent the total PDF (solid line), total background (dashed line), combinatorial background plus peaking background B described in the text (dot-dashed line), and combinatorial background only (dotted line). In (a)–(c), the middle two curves overlap because the peaking background A is negligible.

particles j in the event, where θ_j^* and p_j^* are the angle with respect to the B^0 thrust and the momentum in the c.m. frame. Different cuts on $\mathcal{F}$ are applied for each mode to optimize the signal significance based on simulated event samples. Candidates used in the subsequent fits have beam-energy substituted mass $m_{\rm ES} = \sqrt{(\sqrt{s}/2)^2 - (p^*)^2} > 5.2\ {\rm GeV}/c^2$ and energy difference $|\Delta E| = |E^* - \sqrt{s}/2| < 150$ MeV, where E^* and p^* are the energy and momentum of the B^0 candidate and $\sqrt{s}$ is the total energy in the c.m. frame.

We study five samples separately: (a) $B^0 \to \bar{D}^0 K^+ \pi^-$ excluding the $D^{*-}K^+$ contribution, (b) $B^0 \to D^0 K^+ \pi^-$, (c) $B^0 \to \bar{D}^0 K^*(892)^0$, (d) $B^0 \to D_2^*(2460)^- K^+$, and (e) $B^0 \to D^{*-} h^+$, where h^+ is a pion or kaon. Samples (c) and (d) are subsets of (a), where the resonances are selected within 1.5 times their full widths [12].

For samples (a)–(d), a two-dimensional ($m_{\rm ES}$, ΔE) unbinned-maximum-likelihood fit is used to determine the signal yields. The signal component is the product of a Gaussian in $m_{\rm ES}$ centered at the B^0 mass and a Crystal Ball line shape [15] in ΔE centered near zero. The combinatorial background component is modeled with an Argus threshold function [16] in $m_{\rm ES}$ and a second-order polynomial in ΔE. Two background components peak in $m_{\rm ES}$: peaking background A describes the $B^0 \to D^{**-}\pi^+$ contribution, which also peaks in ΔE but the peak is shifted by about +50 MeV because the pion is misidentified as a kaon; peaking background B uses a second-order polynomial in ΔE to accommodate events such as $D^{(*)}K^{(*)}\pi$, and $D^{(*)}\rho$, where one or more pions or photons are missed in the reconstruction and/or a pion is misidentified as a kaon. The probability density function (PDF) is the sum of the signal and three background components. A large $B^0 \to D^{*-}\pi^+$ data control sample is used to determine the signal shape in both ΔE and $m_{\rm ES}$, and the peaking background A in ΔE, where we assign the kaon mass to the pion candidate. We use the same parameters for signal and peaking backgrounds in $m_{\rm ES}$ since they are consistent in simulation. The ΔE distributions and yields for the four components in the signal region are shown in Fig. 1 and Table I, respectively.

The signal yield for $B^0 \to \bar{D}^0 K^+ \pi^-$ is corrected for variations in signal efficiency across the $DK\pi$ Dalitz plot. Each event k with variables $\vec{q}_k \equiv (m_{{\rm ES},k}, \Delta E_k)$ is assigned a signal weight [17]

$$w_{\rm sig}(\vec{q}_k) = \frac{\sum_{j=1}^4 V_{{\rm sig},j} P_j(\vec{q}_k)}{\sum_{j=1}^4 N_j P_j(\vec{q}_k)},$$

calculated from the four PDF components P_j, their yields N_j from the fit, and the covariance matrix elements $V_{{\rm sig},j}$ between $N_{\rm sig}$ and N_j. The efficiency-corrected signal yield is then $\sum_k w_{\rm sig}(\vec{q}_k)/\varepsilon_k$, where the efficiency ε_k is estimated from the simulated events in the vicinity of each data point in the Dalitz plot.

Figure 2 shows the signal weight distribution as a function of $m_{K^+\pi^-}$ and $m_{\bar{D}^0\pi^-}$. The peaks near $m_{K^*(892)^0}$ and $m_{D_2^*(2460)^-}$ are clearly visible. We use the ($m_{\rm ES}$, ΔE) fit

TABLE I. The yields of signal, combinatorial (comb.), and peaking (peak A, peak B) background PDFs of the samples (a)–(d) described in the text; values and errors are rescaled to represent the yields in the signal region ($m_{\rm ES} > 5.27\ {\rm GeV}/c^2$, $|\Delta E| < 40$ MeV). The bottom row shows the branching fractions with statistical errors.

	(a) $B^0 \to \bar{D}^0 K^+ \pi^-$			(b) $B^0 \to D^0 K^+ \pi^-$			(c) $B^0 \to \bar{D}^0 K^*(892)^0$			(d) $B^0 \to D_2^*(2460)^- K^+$		
D^0 mode	$K\pi$	$K\pi\pi^0$	$K\pi\pi\pi$	$K\pi$	$K\pi\pi^0$	$K\pi\pi\pi$	$K\pi$	$K\pi\pi^0$	$K\pi\pi\pi$	$K\pi$	$K\pi\pi^0$	$K\pi\pi\pi$
Signal	101 ± 17	58 ± 20	69 ± 19	-17 ± 13	34 ± 24	8 ± 22	35 ± 7	21 ± 7	31 ± 7	15 ± 6	15 ± 6	16 ± 5
Comb.	229 ± 4	500 ± 5	528 ± 5	608 ± 5	918 ± 6	989 ± 6	17 ± 1	29 ± 1	30 ± 1	16 ± 1	16 ± 1	22 ± 1
Peak A	5 ± 6	0 ± 1	0 ± 2	0 ± 0	0 ± 0	0 ± 0	0 ± 0	0 ± 0	0 ± 0	2 ± 2	5 ± 2	2 ± 1
Peak B	45 ± 9	76 ± 12	42 ± 10	50 ± 11	54 ± 14	45 ± 13	6 ± 3	10 ± 3	3 ± 3	2 ± 3	7 ± 3	0 ± 1
$\mathcal{B}(10^{-6})$		88 ± 15			-4 ± 12			38 ± 6			18.3 ± 4.0	

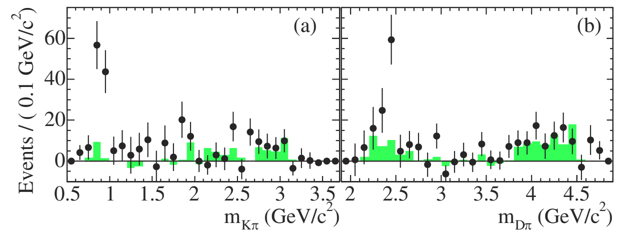

FIG. 2 (color online). The signal weight distribution as a function of $m_{K^+\pi^-}$ and $m_{\bar{D}^0\pi^-}$. The shaded histograms include only events with (a) $|m_{\bar{D}^0\pi^-} - 2460\ \text{MeV}/c^2| < 75\ \text{MeV}/c^2$, and (b) $|m_{K^+\pi^-} - 896\ \text{MeV}/c^2| < 150\ \text{MeV}/c^2$.

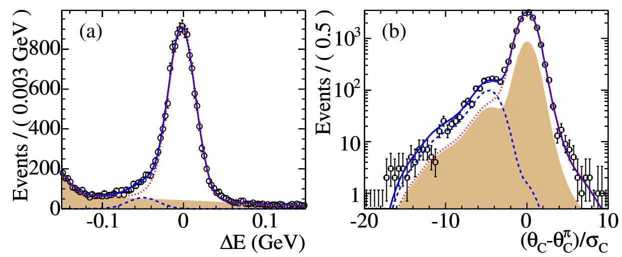

FIG. 3 (color online). (a) ΔE and (b) Cherenkov angle $(\theta_C - \theta_C^\pi)/\sigma_C$ distributions for $D^{*-}h^+$ candidates and PDF projections. Circles with error bars are data points. Shaded distribution is the combinatorial background, the dotted curve adds the $D^*\pi$ contribution, and the solid curve is the full PDF. The dashed curve represents the D^*K contribution only. ΔE for $D^*\pi$ is centered near zero, while for D^*K it is shifted to lower values because the prompt track is assumed to be a pion.

results and signal efficiencies estimated from simulated $B^0 \to \bar{D}^0 K^*(892)^0$ and $B^0 \to D_2^*(2460)^- K^+$ samples to compute corresponding branching fractions. For the $B^0 \to D^0 K^+ \pi^-$ mode, we assume a flat distribution on the Dalitz plot when determining the signal efficiency.

For modes in which we do not observe a significant signal, the 90% confidence level (C.L.) branching fraction upper limit (UL) is determined by integrating the product of the PDFs for the three D^0 modes as a function of branching fraction from 0 to $\mathcal{B}_{\text{UL}}$ so that $\int_0^{\mathcal{B}_{\text{UL}}} \mathcal{L} d\mathcal{B} = 0.9 \int_0^\infty \mathcal{L} d\mathcal{B}$, where $\mathcal{L}$ is the likelihood function.

To measure r, we select events with $m_{\text{ES}} > 5.27\ \text{GeV}/c^2$ from sample (e). A two-dimensional PDF of ΔE and θ_C (the reconstructed Cherenkov-light angle of the prompt track) is used to separate D^*K from $D^*\pi$ decays. Tracks with an estimated θ_C uncertainty $\sigma_C > 4$ mrad or $n_{\gamma,s}/\sqrt{n_{\gamma,s} + n_{\gamma,b}} < 3$ are removed, where $n_{\gamma,s}$ and $n_{\gamma,b}$ are the numbers of signal and background photons determined from a likelihood fit to the ring of Cherenkov photons associated with the track [11]. Finally, events are rejected if θ_C is smaller than the predicted Cherenkov angle for kaons by more than $4\sigma_C$, in order to remove particles heavier than kaon.

The ΔE signal peak PDF is a Crystal Ball line shape and the background is a linear function plus a Gaussian peaked near -150 MeV to accommodate background events such as $D^*\rho$ and $D^{**}\pi$ where a soft π is missed in the reconstruction.The distribution of $(\theta_C - \theta_C^\pi)/\sigma_C$ is modeled by Gaussian functions. For the pion component, we use three Gaussian functions centered near zero. For the kaon component, a single Gaussian function centered near $(\theta_C^K - \theta_C^\pi)/\sigma_C$ is sufficient, where θ_C^K and θ_C^π are the expected Cherenkov angle for kaon and pion, respectively, based on the measured momentum. Most of the parameters are obtained from a fit to the pion or kaon tracks in a large $c\bar{c} \to D^*X \to D^0\pi X$, $D^0 \to K^-\pi^+$ data control sample, except the total width of the distribution, which is free in the final fit to accommodate a small difference in width due to differences in momentum spectra between signal and control samples.

Figure 3 shows the ΔE and $(\theta_C - \theta_C^\pi)/\sigma_C$ distributions and PDF projections for $B^0 \to D^{*-}h^+$ ($h = \pi$ or K) candidates. We find 13 400 signal events, of which $f = (6.80 \pm 0.28)\%$ are D^*K events, and 4850 background events in the sample. The ratio $r = f/(1 - f)$ is corrected by the signal efficiency ratio $r_\varepsilon = \varepsilon_{D^*}K/\varepsilon_{D^*}\pi = (94.0 \pm 2.3)\%$ obtained from simulation. This ratio is smaller than unity because θ_C for kaons is smaller (resulting in fewer Cherenkov photons) and more kaons than pions decay in flight within the tracking volume. The uncertainty on r_ε includes simulation statistics and systematic uncertainties due to the two aforementioned effects.

For samples (a)–(d), the systematic uncertainties on the signal efficiency are studied with large τ lepton decay samples (for track reconstruction efficiency) and comparisons between signal simulation and the $B^0 \to D^{*-}\pi^+$ data control sample. The fractional uncertainty, common to all four samples, on signal efficiency is 5% including the uncertainties on the number of $B\bar{B}$ events and the D^0 branching fractions. For the $B^0 \to \bar{D}^0 K^+\pi^-$ mode, the uncertainty of efficiency variation on the Dalitz plot contributes an additional systematic error of 8%. In addition, we vary the control sample shapes in each fit by one standard error and sum the changes in signal yield in quadrature. The total signal yield variations are 8, 2.0, 3.4, and 2.6 events for $\bar{D}^0 K^+\pi^-$, $D^0 K^+\pi^-$, $\bar{D}^0 K^*(892)^0$, and $D_2^*(2460)^- K^+$, respectively. For the $B^0 \to \bar{D}^0 K^*(892)^0$ and $D_2^*(2460)^- K^+$ measurements, we consider possible contamination from each other and from the nonresonance contribution. Using the signal yields for $B^0 \to \bar{D}^0 K^*(892)^0$ and $D_2^*(2460)^- K^+$, and the cross-feed efficiencies determined from simulation, we find that six events in each of these two B^0 modes could be attributed to the other mode and to nonresonance contributions. This contributes a 6% uncertainty for $B^0 \to \bar{D}^0 K^*(892)^0$ and 11% for $B^0 \to D_2^*(2460)^- K^+$. The uncertainty due to the full width of the $D_2^*(2460)^-$ and $K^*(892)^0$ resonances is 8% for $B^0 \to D_2^*(2460)^- K^+$ and less than 1% for $B^0 \to \bar{D}^0 K^*(892)^0$.

The largest systematic uncertainties cancel in the branching ratio measurement [sample (e)]. The remaining systematic errors are from PDF shapes, control sample distributions and contaminations (1.9%), residual uncertainties in the signal efficiency ratio (2.4%), and potential fit bias (2.1%). The last item has been evaluated with simulation samples including background.

In conclusion, we have measured the branching fraction for the $B^0 \to \bar{D}^0 K^+ \pi^-$ decay excluding $D^{*-} K^+$,

$$\mathcal{B}(B^0 \to \bar{D}^0 K^+ \pi^-) = (88 \pm 15 \pm 9) \times 10^{-6},$$

as well as its two significant resonances,

$$B(B^0 \to \bar{D}^0 K^*(892)^0) \times B(K^*(892)^0 \to K^+ \pi^-) = (38 \pm 6 \pm 4) \times 10^{-6},$$

and

$$B(B^0 \to D_2^*(2460)^- K^+) \times B(D_2^*(2460)^- \to \bar{D}^0 \pi^-) = (18.3 \pm 4.0 \pm 3.1) \times 10^{-6}.$$

The signal significances are 8.7, 8.3, and 5.0 standard deviations, respectively, determined from the change in the likelihood between the best fit and a fit with the signal yield fixed to zero (the first case) or the possible cross feed from other sources (six events for the latter two cases). From a fit excluding the observed resonances, assuming flat distriubtion on the Dalitz plot, we find $\mathcal{B}(B^0 \to \bar{D}^0 K^+ \pi^-) = (26 \pm 8 \pm 4) \times 10^{-6}$, whose signal significance is 3.1σ and 90% confidence level upper limit is 37×10^{-6}. We do not observe a significant signal for the CKM-suppressed $B^0 \to D^0 K^+ \pi^-$ mode. The 90% confidence level upper limit is $\mathcal{B}(B^0 \to D^0 K^+ \pi^-) < 19 \times 10^{-6}$. The event yields in this channel are lower than anticipated [5], indicating that a significantly larger data sample is required to constrain γ through this method.

The ratio of branching fractions for $B^0 \to D^{*-} K^+$ to $B^0 \to D^{*-} \pi^+$ is measured to be

$$r = (7.76 \pm 0.34 \pm 0.29)\%,$$

a nearly fourfold improvement compared to the previous result [8]. This ratio is consistent with $(f_K/f_\pi)^2 \tan^2\theta_{\text{Cab}} \simeq 0.072$ [18], expected at tree level if factorization and flavor-SU(3) symmetry hold, where θ_{Cab} is the Cabibbo angle and f_K and f_π are the decay constants of the kaon and pion, respectively.

We are grateful for the excellent luminosity and machine conditions provided by our PEP-II colleagues, and for the substantial dedicated effort from the computing organizations that support *BABAR*. The collaborating institutions wish to thank SLAC for its support and kind hospitality. This work is supported by DOE and NSF (USA), NSERC (Canada), IHEP (China), CEA and CNRS-IN2P3 (France), BMBF and DFG (Germany), INFN (Italy), FOM (The Netherlands), NFR (Norway), MIST (Russia), and PPARC (United Kingdom). Individuals have received support from CONACyT (Mexico), A. P. Sloan Foundation, Research Corporation, and Alexander von Humboldt Foundation.

*Also at Dipartimento di Fisica, Università di Perugia, Perugia, Italy.
†Also at Università della Basilicata, Potenza, Italy.
‡Deceased.

[1] N. Cabibbo, Phys. Rev. Lett. **10**, 531 (1963); M. Kobayashi and T. Maskawa, Prog. Theor. Phys. **49**, 652 (1973).
[2] M. Gronau and D. Wyler, Phys. Lett. B **265**, 172 (1991).
[3] D. Atwood, I. Dunietz, and A. Soni, Phys. Rev. Lett. **78**, 3257 (1997).
[4] A. Giri, Y. Grossman, A. Soffer, and J. Zupan, Phys. Rev. D **68**, 054018 (2003).
[5] R. Aleksan, T. C. Petersen, and A. Soffer, Phys. Rev. D **67**, 096002 (2003).
[6] M. Gronau, Phys. Lett. B **557**, 198 (2003).
[7] The charge conjugate state is implied throughout this Letter.
[8] K. Abe *et al.* (BELLE Collaboration), Phys. Rev. Lett. **87**, 111801 (2001).
[9] P. Krokovny *et al.* (BELLE Collaboration), Phys. Rev. Lett. **90**, 141802 (2003).
[10] B. Aubert *et al.* (BABAR Collaboration), Nucl. Instrum. Methods Phys. Res., Sect. A **479**, 1 (2002).
[11] I. Adam *et al.* (BABAR DIRC Collaboration), Nucl. Instrum. Methods Phys. Res., Sect. A **538**, 281 (2005).
[12] S. Eidelman *et al.* (Particle Data Group), Phys. Lett. B **592**, 1 (2004).
[13] G. Fox and S. Wolfram, Phys. Rev. Lett. **41**, 1581 (1978).
[14] P. L. Frabetti *et al.* (E687 Collaboration), Phys. Lett. B **331**, 217 (1994).
[15] The Crystal Ball line shape is a modified Gaussian distribution with a transition to a tail function on one side $[(n/\alpha)^n \exp(-\alpha^2/2)]/((\bar{x} - x)/\sigma + n/\alpha - \alpha)^n$ when $x \leq \bar{x} - \alpha\sigma$, where $\bar{x}$ and σ are the mean and width of the Gaussian for $x > \bar{x} - \alpha\sigma$.
[16] H. Albrecht *et al.* (ARGUS Collaboration), Phys. Lett. B **185**, 218 (1987).
[17] M. Pivk and F. R. Le Diberder, Nucl. Instrum. Methods Phys. Res., Sect. A **555**, 356 (2005).
[18] The value is calculated from $\Gamma(\tau^- \to K^- \nu_\tau)/\Gamma(\tau^- \to \pi^- \nu_\tau)$, corrected for phase space factors.